

## NUMERICAL INVESTIGATION OF HEAT TRANSFER IN A SPENT NUCLEAR CASK

<sup>[1]</sup>D.K.Ramesha, <sup>[2]</sup>Dayanandachari K V, <sup>[2]</sup>Trilok G,  
<sup>[2]</sup>Vinay Kumar Reddy V

<sup>[1]</sup>Associate Professor, <sup>[2]</sup>PG Scholar,

Department of Mechanical Engineering, University Visvesvaraya College of Engineering,  
Bangalore University, Bengaluru-560001, Karnataka, India

---

### Abstract

The spent fuel continues to generate heat, there is a need to know whether the temperatures reached during shipping and storage are within the safety limits in fast breeder reactors. The scope of work includes CFD analysis of the shipping cask for obtaining flow and temperature distributions for specified heat generation rates for the fuel rods in rhombus sheath. Two-dimensional heat exchange by pure convection, heat transfer coupled with pure convection and thermal radiation of spent nuclear cask are considered. Geometric modelling was done using gambit and numerical analysis was carried out for natural convection environment using commercial CFD software fluent. Results for the dimensionless maximum temperature versus heat generation rate are obtained and compared with the isotherm, velocity streamline flow for various Grashoff number.

**Keywords:** Nuclear cask, shell, cladding, fuel rod, spent fuel

---

### 1. INTRODUCTION

The increasing energy demand and the total dependence on the fossil fuel for the energy generation can be substantially reduced by perceiving nuclear energy as an attractive stable energy generation technology while valuing the environmental concerns as a result there is need to study the nuclear energy in all dimensions.

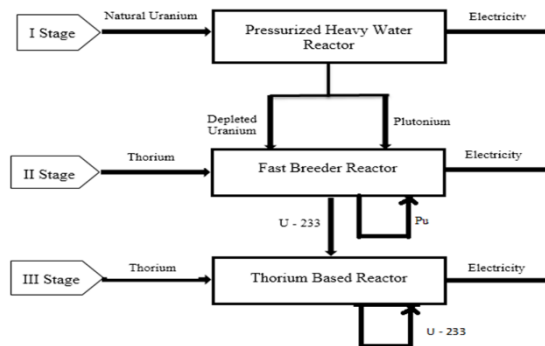


Fig 1.1: Flow chart of heat transfer mechanisms and spent nuclear cask

### Spent Fuel Nuclear Cask:

The fuel inside the reactor core which undergoes reaction after sometime becomes inefficient to carry out reactions further. Such fuel is named as spent fuel. The subassemblies may have circular, rhombus or hexagonal cross section. A typical fuel subassembly contains several fuel rods which varies from as low as 3x3, 4x4. Once the reaction begins the fuel inside the assemblies becomes less effective over period of time. Hence the spent nuclear fuels are transferred from the reactor zone to the storage zone. The spent fuel coated with zircalloy of suitable thickness is loaded into a pot which is leak proof and also filled with argon gas. Then the pot is placed concentrically inside an enclosure having a thick wall called spent nuclear storage cask. Lead or concrete material is used for building the walls of the cask.

### Heat Transfer Processes in Spent Fuel Nuclear Cask

In this particular problem the heat generating rods are placed in a sheath of rhombus cross section. The rods are coated. Circumferentially by a small thickness called cladding. The space between the rods contains a backfill gas like argon, helium etc. The volumetric heat generation in rods drives the natural convection and radiation in the space between rods and enclosure respectively. Based on the Rayleigh number critical value, the convection or conduction may take place in the backfill gas. If the Rayleigh number is greater than the critical value then convection takes place. Radiation takes place from rod to rod surface, rod and the outside sheath surface simultaneously along with the conduction and convection. In rhombus sheath contain 16 spent fuel rods bundle filled with argon gas and sealed and all are bolted together and finally air is filled completely inside the cylindrical cask and sealed at either ends.

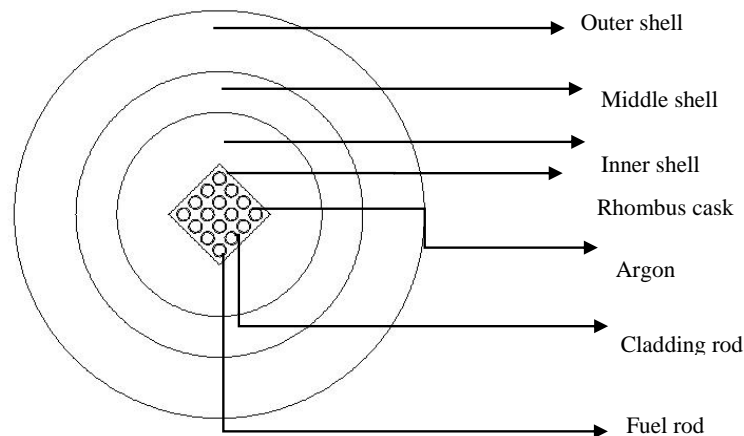


Fig 1.2: Flow chart of heat transfer mechanisms & spent nuclear cask

## 2. LITERATURE REVIEW

Canaan and Klein [1] experimentally studied the rhombus rod bundle of size 8 x 8 with ratio of pitch-to-diameter about 1.33 for back fill gases of helium and nitrogen. Correlation were developed for Nusselt number in conduction and convection regimes relating total convection power, maximum temperature and average assembly temperature were presented for both the regimes. Keyhani and Dalton [2] studied experimentally on free convection in enclosed horizontal N x N arrays varying N of 3 to 7 electrically heated rods for 1.35 pitch-to-diameter. Pressurized air or helium was used as the working fluid. Nusselt number is correlated with the array size, N as the function of modified Rayleigh number and this correlation may be readily used to obtain a conservative estimate of maximum temperature. Hung and Cheng [3] experimentally studied effect of pressure in natural/free convection for the fluid like non-Boussinesq fluid in the enclosure of rectangular geometry. Determined the density, absolute pressure, and temperature & velocity distributions. The equations of a staggered grid, equivalent modified Ra ranging from 104 to 106. They conclude that the enclosure exert great influence on the flow and thermal field. Keyhani and Fulacki [4] experimentally investigated free convection for two vertical, enclosed rod bundles for a wide range of Rayleigh number. The specific power dissipation maintained at constant temperature. Nusselt number for each rod is obtained by Rayleigh number. The water results

obtained at high Rayleigh number yields nearly the same heat transfer coefficient for the 3x3rods in the bundle. Kuehn and Goldstein [5] experiment carried out for free convection. The natural convection occurs in annuli of the concentric and eccentric horizontal space and the comes to conclusion that the overall heat transfer results obtained using air with inner cylinder placed eccentrically by  $\epsilon/L = 2/3, 1/3, -2/3, -1/3$  observed that restriction of the flow and the overall heat transfer coefficients varied less than 10 percent of that of the concentric case. Beckman [6] carried out the study of the free convection. This natural convection occurs in gap/space between the two concentric cylinders placed horizontally and these cylinders are maintained at constant temperature. The fluids used in these experiments are hydrogen, air, and carbon dioxide to find out the overall heat transfer coefficient. Boyd [7] experimental studies of natural/free convection which occurs in the region/annular space between the cylinders of hexagonal size and the outer circular shape with inner heat generating using Mach-Zehnder interferometer for various gases like air, neon, helium, krypton, argon, xenon and it is observed that laminar flow is steady in lower half and unsteady in upper half at the Rayleigh number  $Ra \geq 8.15 \times 10^2$ . the spacing between the isotherms reduced as the hexagon approached from normal direction due to increase in temperature gradient or heat flux, gave correlation between  $Ra$  and average Nusselt number  $Nu_{avg} = 0.794 Ra^{0.25}$  Kim and Viskanta [8] performed calculations for coupled conduction. Convection and surface radiation indicate that the heat transfer by natural convection decreases due to radiation coming into play. The computed and measured temperature distributions are in very good agreement in respect of walls, although a fair agreement is found in respect of the fluid. Lageet al. [9] have also performed combined convection and surface radiation calculations using simplified model and assuming that the top is a black isothermal surface at the temperature  $T_{\infty}$  and that the cold wall and the bottom of the cavity together form an adiabatic surface. These calculations show that an increase in the emissivity's (hot and cold) and a decrease in the aspect ratio  $H/L$  (from 1 to 1.25), both result in an increase in the adiabatic surface temperature. Also the relative contribution of radiation compared to convection, increases with  $T_h$  and decreases with  $H/L$ . Balaji and Venkateshan [10] in the study of the interaction of surface radiation with free convection in a differently heated rhombus enclosed space with isothermal vertical & adiabatic horizontal walls have found that surface radiation varies with overall heat transfer compared to pure natural convection case. Compared pure natural convection results obtained from analytical or numerical investigations with those obtained from the experiments by subtracting the radiation component from the overall heat transfer. Balaji and Venkateshan [11] have found that the convection and radiation can be assumed to be decoupled and that the two Nusselt numbers for the cavities of the aspect ratio a greater than 2 can be calculated from the relations. Baek et al. [12] carried out 3D computational study on a small finite thickness heat generating element. The authors have shown that the substrate thermal conduction, radiation and the emissivity of the walls all have significant effect upon the temperature rise of the heater. Mezrhab et al. [13] have studied the effect of a centrally placed rhombus solid on the radiation interaction with natural/free convection in a rhombus cavity. They have concluded that the presence of the solid did not

influence the pure convective heat transfer but had the effect of increasing combined mode of heat transfer across the cavity at high Ra numbers and high solid-to-fluid thermal conductivity. Xaman et al. [14] have studied radiation combined with the turbulent and laminar free convection in a cavity with adiabatic horizontal boundaries, a thick glass vertical wall and an isothermal vertical wall. The present study considers all mode of heat transfer processes and involves laminar conjugate heat transfer in a spent nuclear fuel cask of a fast breeder reactor with a heat generating rod bundle containing sixteen rods, with the bundle placed symmetrically at the centre of the cask within a sheath.

### 3. PHYSICAL MODEL AND MATHEMATICAL FORMULATION

A 2-D analysis is carried out considering the cross-section of the FSA (Fuel Sub-Assembly), which consists partly of argon gas and partly the cross-sections of the heat generating rods. For the geometry considered, X and Y axes taken in the horizontal and vertical directions. Each side of the rhombus sheath has length  $d = 35\text{mm}$ . The dimensions of the inner shell are  $r_1=44\text{ mm}$  and  $r_2=94\text{ mm}$ , outer shell are  $r_2 = 94\text{ mm}$  and  $r_3=188\text{mm}$ . It may be noted that the outer diameter of inner shell is same as the inner diameter of the outer shell, the fluid flow in annulus space is quiescent at time interval  $\leq \text{zero}$ , and the temperature of fluid,  $T_{\text{ref}}$  is constant. And time interval  $\geq \text{zero}$ , generation of heat starts in the fuel rods and this heat generation is uniform with compare to the rate of volumetric heat generation,  $Q_v$ . The heat generated is transferred by conduction inside the rods and across the zircalloy cladding surrounding the fuel rods and then by natural convection into the backfill gas (which is argon here). Part of the heat transfer from the cladding surfaces also occurs by radiation to the inner surface of the rhombus sheath by radiation. It is assumed here that the outer shell boundary is maintained at constant temperature  $T_c$ .

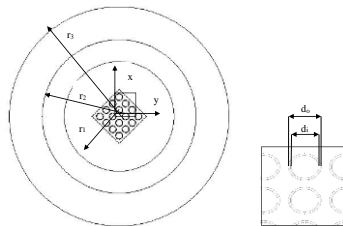


Fig3.1: Physical modelling and coordinate system considered for 2D analysis

### Governing equations

Here the fluid considered is air. Since the problem involves high temperatures, low pressures and the fluid is compressible hence here ideal gas equation is employed with low Mach number approximation. Boussinesq model can become insufficient to this kind of problems as only density variation is the function of temperature and density is only taken into account in the body force terms.

### Low Mach number approximation

For the compressible flow problems there exists sound wave propagation, as the mach number is solely responsible for the characteristic speed amongst Rayleigh number, Froude number and Peclet number, if the sound wave travels more than one cell when the pressure forces are travelling only one cell per each time step then the sound waves are going to affect the solution adversely. Hence there is a need to filter out the acoustic sound waves that propagate in the compressible flow problems since there is no need to know about the sound wave behaviour in the heat transfer problems. Thus the sound wave propagation should be eliminated or the effect should be diminished so that it will not have any influence on the final results, as the mach number approaches zero the acoustic waves get uncoupled from the momentum and energy equations which actually vanishes this is because as the mach number is reduced the hyperbolic equation becomes elliptical equation and thus acoustic waves now travel at infinite speed and their effects disappear from the equations. Thus the usage of low Mach number approximation is beneficial to solve this kind of heat transfer problems, which results in the following formulation:

$$\frac{\partial}{\partial t}(\rho\phi) + \frac{\partial}{\partial x}(\rho u\phi) + \frac{\partial}{\partial y}(\rho v\phi) = \frac{\partial}{\partial x}\left(\Gamma\phi\frac{\partial\phi}{\partial x}\right) + \frac{\partial}{\partial y}\left(\Gamma\phi\frac{\partial\phi}{\partial y}\right) + S\phi \quad 3.1$$

For the continuity equation,  $\phi=1$ ,  $\Gamma\phi=0$  and  $S\phi=0$

$$\frac{\partial\rho}{\partial t} + \frac{\partial}{\partial x}(\rho u) + \frac{\partial}{\partial y}(\rho v) = 0 \quad 3.2$$

$$\frac{\partial}{\partial t}(\rho u) + \frac{\partial}{\partial x}(\rho uu) + \frac{\partial}{\partial y}(\rho vu) = \frac{\partial}{\partial x}\left(\eta \frac{\partial u}{\partial x}\right) + \frac{\partial}{\partial y}\left(\eta \frac{\partial u}{\partial y}\right) + S_u \quad 3.3$$

For the X direction momentum equation,  $\phi=u$ ,  $\Gamma\phi=\eta$  and  $S\phi=S_u$

$$S_u = \frac{\partial}{\partial x}\left(\eta \frac{\partial u}{\partial x}\right) + \frac{\partial}{\partial y}\left(\eta \frac{\partial v}{\partial x}\right) - \frac{\partial}{\partial x}\left(\frac{2}{3}\eta D\right) - \frac{\partial p_1}{\partial x} + (\rho - \rho_c)g\hat{g} \cdot \hat{i} \quad 3.4$$

For the Y direction momentum equation,  $\phi=v$ ,  $\Gamma\phi=\eta$  and  $S\phi=S_v$

$$\frac{\partial}{\partial t}(\rho v) + \frac{\partial}{\partial x}(\rho uv) + \frac{\partial}{\partial y}(\rho vv) = \frac{\partial}{\partial x}\left(\eta \frac{\partial v}{\partial x}\right) + \frac{\partial}{\partial y}\left(\eta \frac{\partial v}{\partial y}\right) + S_v \quad 3.5$$

$$S_v = \frac{\partial}{\partial x}\left(\eta \frac{\partial u}{\partial x}\right) + \frac{\partial}{\partial y}\left(\eta \frac{\partial v}{\partial y}\right) - \frac{\partial}{\partial y}\left(\frac{2}{3}\eta D\right) - \frac{\partial p_1}{\partial y} + (\rho - \rho_c)g\hat{g} \cdot \hat{j} \quad 3.6$$

For the energy equation of fluid,  $\phi=T$ ,  $\Gamma\phi=\lambda/C_p$  and  $S\phi=S_f$  ( $C_p$  is taken as constant)

$$\frac{\partial}{\partial t}(\rho T) + \frac{\partial}{\partial x}(\rho uT) + \frac{\partial}{\partial y}(\rho vT) = \frac{\partial}{\partial x}\left(\frac{\lambda}{C_p} \frac{\partial T}{\partial x}\right) + \frac{\partial}{\partial y}\left(\frac{\lambda}{C_p} \frac{\partial T}{\partial y}\right) S_{e, f} \quad 3.7$$

$$S_{e, f} = \frac{T\beta dp_0}{C_p dt} \quad 3.8$$

The energy equation for the solid is derived from the fluid by making X and Y velocities 0. Here  $\phi=T_s$ ,  $\Gamma\phi=\lambda_s/C_s$  and  $S\phi=S_{e,s}$ .

$$\frac{\partial}{\partial t} (\rho_s T_s) = \frac{\partial}{\partial x} \left( \frac{\lambda_s \partial T}{c_s \partial x} \right) + \frac{\partial}{\partial y} \left( \frac{\lambda_s \partial T}{c_s \partial y} \right) + S_{e,s} \quad 3.9$$

$$S_{e,s} = \frac{Q_y}{c_s} \quad 3.10$$

In the above equations u, v and are x-y velocities respectively. The quantity  $\phi$  is a generic variable and  $S\phi$  is the source term for the convection and diffusion equation of  $\phi$ . For generality, the source term  $Q_v$  can be taken to be spatially and even temporarily varying, The equation of state for the working medium relates the density and the temperature to the zeroth order pressure via the ideal gas equation, as follows:

$$p_0 = \rho RT \quad 3.11$$

Where  $\rho$  and  $R$  are the density and the characteristic gas constant. When the ideal gas approximation is made, the term  $T/\beta$  in the energy equation for the fluid may be taken as unity. The pressure is the sum of the zeroth order pressure  $p_0$  and the local first order pressure excess over the hydrostatic. Denoting the local first order pressure as  $p_1$ , and hydrostatic pressure as  $p_h$ , it can be stated that:

$$p = p_0 + p_1$$

$$\text{where } p_1 = p_{1,i} + i$$

$$\text{and } p_h = \rho_c [(x - x_c)(\vec{g} \cdot i) + (y - y_c)(\vec{g} \cdot j)] \quad 3.12$$

When  $p_{1,i} = p_h$ , we have  $p_1 = 0$  and  $p = p_0$ , where  $p_0,c$  is the reference zeroth order pressure (i.e. the zeroth order pressure under hydrostatic condition). The quantity  $p_1$ , which is a function of space and time, appears in the momentum equations, and the time derivative of the zeroth order pressure  $dp_0/dt$  appears in the fluid energy equation (in place of the substantive derivative  $Dp/Dt$ ). The zeroth order pressure  $p_0$  is a function of time alone. Hence its gradients do not appear in the momentum equations. The hydrostatic pressure is assigned the value of the reference zeroth-order pressure value  $p_0,c$  at the reference location  $(x_c, y_c)$ .

**Boundary conditions:**

At the beginning of the calculations, the initial conditions for iterations are that fluid inside will be quiescent with uniform temperature. On the boundaries of the fluid, solid and also at the interfaces the velocity in X-direction, the velocity in Y-direction, and the velocity in Z-direction, zero and  $T=T_{ref}$ . Once the calculation begins, fuel rods uniform volumetric heat generation ( $Q_v$ ), the hydrodynamic conditions like no slip and no permeability exist at the outer and inner interfaces. At the interface of inner solid and fluid nearer to inner surface is analyzed by the thermal boundary conditions (denoted by subscript 'isf') are the no heat flux continuity and temperature jump as follows:

$$-k_s \frac{\partial T_s}{\partial n} = -\frac{\partial T_f}{\partial n} + q_{rad,isf}, \quad T_s = T_f \quad 3.13$$

At the outer fluid solid interface (denoted by subscript ofs)

$$-\frac{\partial T_f}{\partial n} = -k_s \frac{\partial T_s}{\partial n} + q_{rad,osf}, \quad T_f = T_s \quad 3.14$$

Where  $q_{rad,isf}$  and  $q_{rad,ofs}$  are the net radiation heat flux leaving the inner interface and outer interface respectively.

**4. METHODOLOGY**

Initially the model is created and mesh is generated in Gambit and then it is imported to Fluent and in Fluent it applicable for control volume. The discretization of the control volume formulated by governing equations. And for this formulation, the SIMPLE algorithm can be used for pressure-velocity coupling. Here SIMPLE stands for Semi-Implicit-Method for Pressure Linked Equation. The SIMPLE is based on the finite volume method and it utilizes the adoptive meshing for calculations of steady state problems. In staggered grid system the pressure, density and temperature are stored at the ordinary nodal points and velocity is found at the staggered nodes. A UDF (User defined functions) is employed for fluids. For the radiation heat transfer surface to surface model is employed with least rhombus method of smoothing which helps to eliminate the round-off errors. Often the Monte Carlo used for validating the results obtained from other meshing techniques as it allows the accurate treatment of spectral properties, inhomogeneous media, anisotropic scattering, complex geometries, and indeed all of the important effects in radiative transfer. Hence Monte Carlo method stands an excellent chance of emerging as the dominant choice for treating radiative heat transfer. The maximum residual of  $10^{-6}$  is considered for convergence check. Input values used for simulation: 50W, 100W, 150W, 200W for fuel rods and 298K for outer walls.

Table 4.1: Zone type and continuum conditions chosen in the analysis

Zone type	Continuum condition	Material used
Outer Shell	Solid	Steel
Middle Shell	Solid	Steel
Inner Shell	Fluid	Air
Rhombus Canister	Fluid	Argon
Cladding Shell	Solid	Zircalloy
Fuel Rod	Solid	Mox

Table 4.2: Material properties

Properties	Fuel	Steel
Density (Kg m <sup>3</sup> )	5000	8030
Specific heat (J Kg-K)	502.4	502.48
Thermal conductivity (W m-K)	1.5	16.27

### Grid sensitivity study:

Grid independency studies are conducted for both conjugate natural convection case and combined convection and radiation mode. 2-D model tests are conducted with 16347, 22197, 31956, 49643 quadrilateral cells with heat generation rates of 100 W and 200W and the results are tabulated for pure conjugate convection & combined conjugate convection and radiation in Table 4.4. For the radiation model emissivity of steel with  $\epsilon = 0.8$  is considered. The percentage imbalance (%imb) is defined as  $[(Q_{gen} - Q_{out}) 100] / Q_{gen}$ , where  $Q_{gen}$  is the rate of heat generation and  $Q_{out}$  is the heat removed at the isothermal boundary. The largest energy imbalance %imb is found to be 0.63129% on examining the results for pure convection and 0.760304% for convection with radiation. It is observed that, there is no considerable change in average temperatures and maximum temperatures. From this we can say that all the grid resolutions mentioned yield acceptable results. For the analysis 44743 cells model is used for the pure convection analysis and 45305 cells model is used for the combined convection and radiation. Grid sensitivity tests for the 2D model are shown in Table 4.4(a), 4.4(b),

Table 4.4(a), 4.4(b): Grid sensitivity

Qgen=100W, Pure Convection			
Cells	Tavg	Qout	%imb
49643	424	99.467	0.46113
31956	424	99.48627	0.4443
22197	423	99.209	0.7284
16347	423.5	99.307	0.7515

Qgen=100W, with Radiation			
Cells	Tavg	Qout	%imb
49643	356.5	99.378	0.5544
31956	356.5	99.3625	0.5603
22197	356.7	99.415	0.5466
16347	356	99.217	0.71523

### Code validation with previously published work:

The results of the Boyd's [7] experimental work have been reproduced using FLUENT v.6.3.26. The problem deals with the experimental study of various heat transfer aspects in the horizontal annulus between concentrically placed circular cylinders inside the hexagonal cylinder. The gas flows in this annulus space and it is flow maintained at the higher temperature. The model was created in Gambit having same dimensions and boundary conditions and total of three different runs were taken by varying the number of cells and noticed that not much variation was identified and finally a model with 14686 quadrilateral cells was used for the present simulation. The values of the average Nusselt number obtained from Fluent and also results which Boyd obtained by varying the Rayleigh number are tabulated in the Figure 4.1.

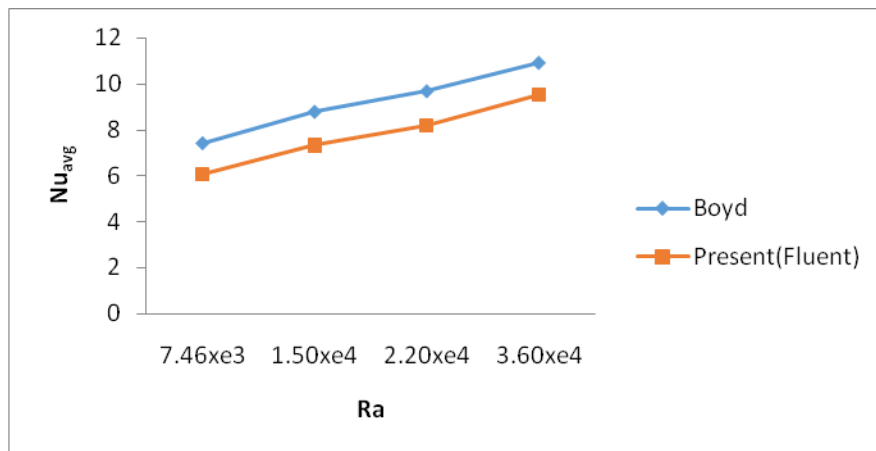


Fig 4.1: Boyd's experimental results compared with the present(Fluent) work

## 5. RESULTS AND DISCUSSION

### Temperature profiles for various heat generation rates:

In this present work, heat generation rate in the spent nuclear cask was studied in the range of 50-200W analysis was carried out at the intervals of 50W for all fuel rods at different time intervals during transportation and storage. The cask outer most surface is maintained at constant temperature 298 K having the air as the working fluid. Since the pressure variation inside the annulus vary between 0.18 Pa to 0.4 Pa only for various heat generation rates up to 200W, so that much attention need not be given on the issue of the build-up of high pressures. From figure 5.1 (a) dimensionless maximum temperature was plotted for varying heat generation rate, from this it can be observed that pure convection have higher temperature ratio compared to coupled heat

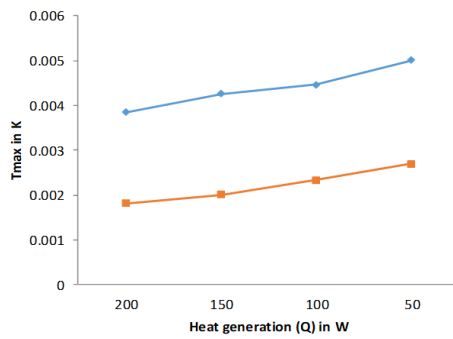
transfer of radiation with convection. Figure 5.1 (b) shows the dimensionless maximum temperature plotted for varying Grashoff number, from this it can be observed that with increase in Grashoff number the dimensionless maximum temperature decreases for both mode of heat transfer. In both the plots it evident that pure convection have higher temperature ratio compared to coupled heat transfer by convection along with radiation, this is because of the increased heat transfer by radiation and convection

#### **Two-Dimensional temperature contour results for pure convection:**

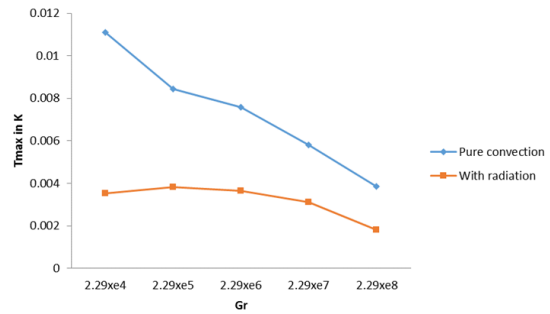
The results of the 2-D analysis done only on spent fuel cross-section region is considered. The heat generation occurs only in the fuel region and tends to be critical area for the analysis. Results are obtained for 50 W-200 W heat generation rates, considering the 16 fuel rods for pure natural convection. In Figure 5.2(a), 5.3(a), only pure natural convection case is considered in which we can observe that the plume is originating centre above the rhombus canister which impinges on the top of the inner wall and moves down gradually from the sides. In the fluid region isotherms we can see lot of variations in the temperature curves inside the annulus in which the V-groove region formed in between the top fuel supply assembly has maximum temperature after which it moves up before it impinges the temperature reduces slightly and once it impinges and moves down gradually the temperature reduces due to heat is transferred to the inner shell due to convection-conductance and once the fluid reaches bottom region the fluid temperature is found to be least. The temperature variations in the inner and outer shells are very less and are almost constant.

#### **Two-Dimensional temperature contour results for conjugate convection with radiation:**

Results are also obtained for 50 W- 200 W heat generation rates, considering the 16 fuel rods for combined conduction, natural convection and radiation. In Figure 5.2(b), 5.3(b) radiation heat transfer has been considered and surface-to-surface radiation comes into play along with natural convection. The isotherm curve pattern is same as that of the natural/free convection in the region of fluid. Here we can observe an interesting thing that there is not much significant change in the fluid temperature. By observing the fluid region and as we move towards the bottom half with reference to the horizontal, the fluid temperature variation is almost nil in the annulus. And also at the centre rhombus formed due to the typical arrangement of the fuel rods placed in the rhombus canister which contains fluid, we can observe that the temperature is lesser than that of the temperature at the core of the rhombus canister whereas in the pure natural convection case both in the rhombus region and the core temperatures are almost the same. This kind of behaviour is due to heat removed by radiation. In this case also there is not much variation in the temperature profiles of the inner and outer steel shells are similar to that of the pure natural convection case. The model in which both natural convection with radiation is considered nearly 60-72% heat is been removed due to only radiation and maximum temperature is always seen inside the rhombus sheaths for both pure natural/free convection and convection along with radiation



5.1(a)



5.1(b)

Fig 5.1(a): Dimensionless maximum temperature vs. Heat generation for pure natural convection case and convection with radiation case

Figure 5.1(b): Dimensionless maximum temperature vs Grashoff number for both pure convection and convection with radiation.

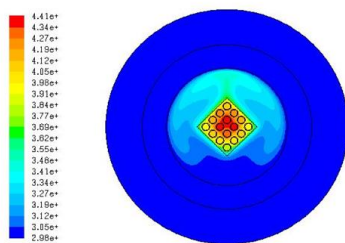


Fig (a)

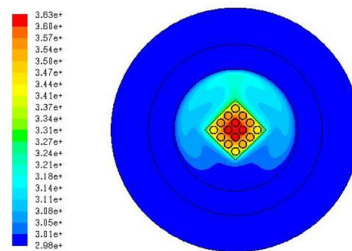


Fig (b)

Fig 5.2: Temperature contours for 50W heat generation in fuel rods (a) Pure natural convection case (b) Convection with radiation case.

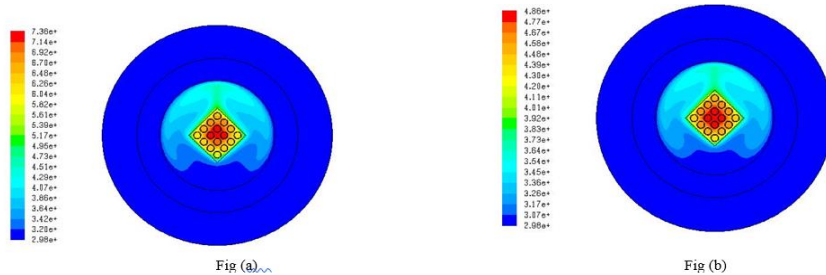


Figure 5.3: Temperature contours for 200W heat generation in fuel rods (g) pure natural convection case (h) Convection with radiation case.

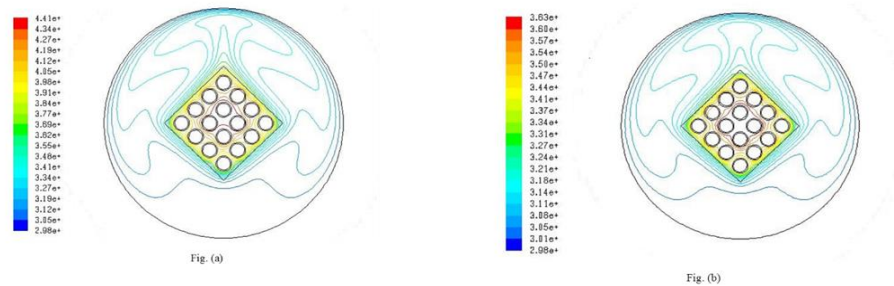


Fig 5.4: Isotherms of 50W heat generation in fuel rods for pure convection (a) and convection with radiation (b)

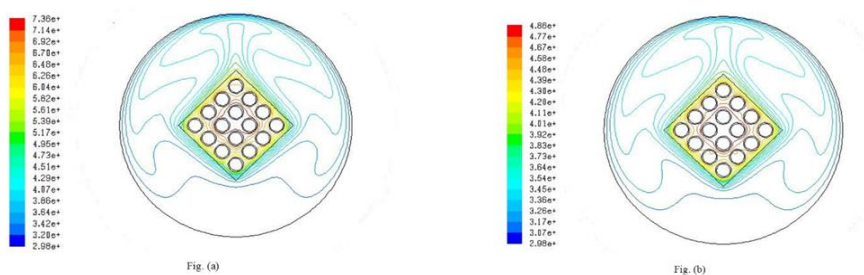


Fig 5.5: Isotherms of 200W heat generation in fuel rods for pure convection (a) and convection with radiation (b).

### Isotherms and Streamlines for Various Grashoff Numbers:

In order to visualize the flow pattern phenomena for both the cases isothermal lines and velocity streamlines were plotted. Hence computations were performed with laminar flow model for

conjugate natural convection and convection with radiation by varying the Grashoff number in the range  $2.29 \times 10^4 - 2.29 \times 10^7$ . Figure 5.6, 5.7, 5.8, and 5.9 the flow and temperature distributions in the form of streamlines and isotherm maps are presented for various Grashoff number choose. In the combined case of convection and radiation the isotherms in the solid region are much denser than with pure convection case rest all other variations are similar to that of the pure natural convection cases shown in Figure. 5.6, 5.7, 5.8 and 5.9. This can be traced to the fact that the temperature in the fluid tends to become homogenized due to the effect of radiation, hence we can see little variations in the temperature contours of the radiation model comparatively. It can be concluded that the effect of radiation is to reduce the intensity of the convective flow.

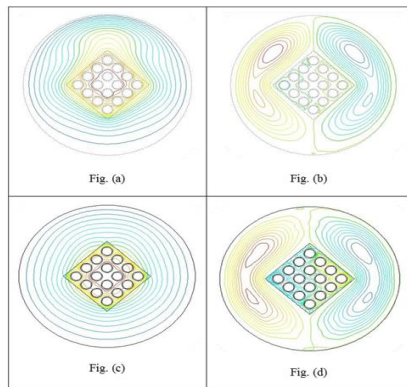


Fig 5.6: For Gr-2.29xe<sup>5</sup>

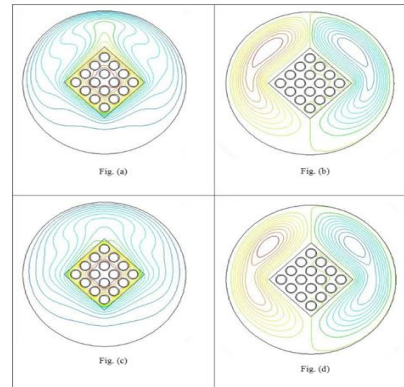


Fig 5.7: For Gr-2.29xe<sup>6</sup>

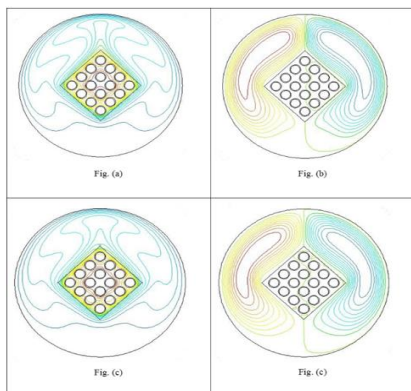


Fig 5.8: For Gr-2.29xe<sup>7</sup>

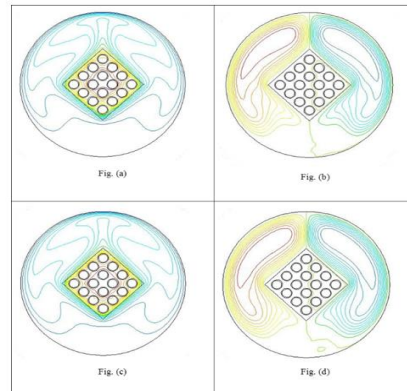


Fig 5.9: For Gr-2.29xe<sup>7</sup>

## 6. CONCLUSION

In this present study numerical investigation was carried for nuclear spent cask for various heat generation rate, grashoff number, plots were drawn for non dimensionless temperature and isothermal, velocity stream line contour were obtained to study the relationship between heat transfer and fluid flow mechanics. The maximum dimensional temperature increases rapidly at initial stages compared to the initial heat generation  $Q$ . The dimensional maximum temperature is always more in the center portion of the rhombus cask in assembly. The inner and outer solid shells have almost constant temperatures for all the cases. The buoyant plume develops vertically above the rhombus cask where as a double plume emerges from the upper corners of rhombus in inclined manner. The maximum temperature always increases as the wattages increases in the domain for the fixed wall temperature. Always stagnant region is maintained at the bottom of the annulus.

## REFERENCES

- [1] Robert E.Canaan and Dale E.Klein, An experimental investigation of natural convection heat transfer within horizontal spent-fuel assemblies, J. Nuclear technology, Vol. 116, 306–317, 1996.
- [2] M. Keyhani and T. Dalton, Natural convection heat transfer in horizontal rod-bundle enclosures, Trans. ASME J. heat transfer, Vol. 118, 598–605, 1996.
- [3] Kuo-Shu Hung and Chin-Hsiang Cheng, pressure effects on natural convection for non-boussinesq fluid in a rectangular enclosure, J. Numerical heat transfer, Vol. 41, 515–528, 2002.
- [4] M. Keyhani, F.A. Kulacki and R.N.Christensen, Experimental investigation of free convection in a vertical rod bundle- A general correlation for Nusselt numbers, J. heat transfer, Vol. 107, 611–623, 1985.
- [5] T.H. Kuehn and R.J. Goldstein, An experimental study of natural convection heat transfer in concentric and eccentric horizontal cylindrical annuli, Trans. ASME J. Heat Transfer Vol. 100, 638–640, 1978.
- [6] Beckmann.W, Die wärmeübertragung in zylindrischen gasschichten bei natürlicher konvektion. Forsch.Geb. d. Ingenieurwesens, Vol. 2 (5), 165–178, 1931.
- [7] Grigull .U and Hauf.W, Natural convection in horizontal cylindrical annuli.Proc. 3rd Int. Heat Transfer Conf, Vol. 2, 154–158, 1966.
- [8] Boyd R.D, Interferometric study of natural convection heat transfer in a horizontal annulus with irregular boundaries, Nucl. Eng. Des, Vol. 83, 105–112, 1984.
- [9] Kim D.M and Viskanta R., Effect of Wall Conduction and Radiation on Natural Convection in a Rectangular Cavity, Numerical Heat Transfer, Vol. 7, 449-470, 1984.
- [10] Lage J.L., Lin J.S and Bejan A., Natural Convection with Radiation in a cavity with open top end, ASME J. Heat Transfer, Vol. 114, 479-486, 1992.

- [11] C. Balaji, S.P. Venkateshan, Interaction of surface radiation with free convection in a rhombus cavity, Int. J. Heat and Fluid Flow, Vol. 14 (3) 260–267, 1993.
- [12] C. Balaji, S.P. Venkateshan, Interaction of Radiation with free convection in an open cavity, Int. J. Heat and Fluid Flow, Vol. 15, 317-324, 1994.
- [13] Baek C, Lee K. and Kim W, Study of Combined Heat transfer in a Three – Dimensional enclosure with a Protruding heat Source, Numerical Heat transfer, Vol. 32, 733-747, 1997.
- [14] Mezrhab A, Bouali H, Amaoui H. and Bouzidi M., Computation of Combined Natural Convection and Radiation Heat Transfer in a Cavity heaving a rhombus Body at its Center, Applied Energy, Vol. 83, 1004-1023, 2006.
- [15] Xaman J, Arce J, Ivarez G. and Chvez Y., Laminar and Turbulent Natural Convection Combined with Surface Thermal Radiation in a rhombus Cavity with a Glass Wall, Int. J. of Thermal Sciences, doi:10.1016/j.ijthermalsci.2008.01.012.
- [16] Kim, H., Kang, G.U. and Cho. C.H., "Comparisons of Peak Cladding Temperature and Effective Thermal Conductivity: CFD Simulation on PWR Spent Fuel Assemblies," WM2016.2016.
- [17] US Government, Licensing Requirements for the Independent Storage of Spent Nuclear Fuel and High Level Radioactive Waste and Reactor-Related Greater than Class C waste. 10 CFR 72, 2014.
- [18] Analysis Of Heat Transfer On Spent Fuel Dry Cask During Short-Term Operations Kim, H.; Lee, D.G.; Kang, G.U.; Cho, C.H.; Kwon, O.J.,2016.
- [19] Kim, H., Kwon, O.J., Kang, G.U. and Lee, D.G., "Comparisons of prediction methods for peak cladding temperature and effective thermal conductivity in spent fuel assemblies of transportation/storage casks," Annals of Nuclear Energy, Vol.71. 2014.
- [20] Ministry of Trade, Industry and Energy(MOTIE), Technology Development of Optimization for Spent Nuclear Fuel Storage and Transportation System, Phase 2 Report. 2014.